Basic Res Cardiol 102: 171–182 (2007)
DOI 10.1007/s00395-006-0628-x

ORIGINAL CONTRIBUTION

Tsung-Ming Lee
Mei-Shu Lin
Chang-Her Tsai
Nen-Chung Chang

Effects of pravastatin on ventricular remodeling by activation of myocardial K_{ATP} channels in infarcted rats: role of 70-kDa S6 kinase

Received: 11 May 2006
Returned for 1. revision: 1 June 2006
1. Revision received: 10 July 2006
Returned for 2. revision: 31 July 2006
2. Revision received: 31 August 2006
Accepted: 19 September 2006
Published online: 13 October 2006

Dr. T.-M. Lee
Cardiology Section,
Dept. of Internal Medicine
Taipei Medical University and Chi-Mei Medical Center
Taipei, Taiwan

M.-S. Lin
Dept. of Pharmacy
National Taiwan University and Hospital
Taipei, Taiwan

C.-H. Tsai
Cardiology Section, Dept. of Surgery
Chi-Mei Medical Center
Tainan, Taiwan

N.-C. Chang (✉)
Cardiology Section, Dept. of Medicine
Taipei Medical University and Hospital
252, Wu-Hsing Street
Taipei, Taiwan
Tel.: +886-2/27372181, ext 3101
Fax: +886-2/23911200
E-Mail: ncchang@tmu.edu.tw

Abstract Reactive cardiomyocyte hypertrophy after myocardial infarction is an important risk factor for arrhythmias. Myocardial ATP-sensitive potassium (K_{ATP}) channels have been implicated in attenuating cardiac hypertrophy by inhibition of 70-kDa S6 kinase. We investigated the effect of pravastatin on ventricular hypertrophy during remodeling after myocardial infarction and whether the attenuated hypertrophic effect was via activation of myocardial K_{ATP} channels. Twenty-four hours after ligation of the anterior descending artery, male Wistar rats were randomized to either vehicle, nicorandil (an agonist of K_{ATP} channels), pravastatin, glibenclamide (an antagonist of K_{ATP} channels), or a combination of nicorandil and glibenclamide or pravastatin and glibenclamide for 4 weeks. Infarct size and mortality were similar among the infarcted groups. Cardiomyocyte sizes isolated by enzymatic dissociation after infarction significantly increased at the border zone in vehicle-treated infarcted rats compared with sham-operated rats. Rats in the nicorandil- and pravastatin-treated groups significantly attenuated cardiomyocyte hypertrophy, as compared with the vehicle-treated group. Arrhythmic scores during programmed stimulation mirrored those of cardiomyocyte hypertrophy. Increased 70-kDa S6 kinase mRNA expression in cardiac remodeling was confirmed by reverse transcription-polymerase chain reaction, consistent with the results of immunohistochemistry and Western blot for the phosphorylation of 70-kDa S6 kinase. Nicorandil-induced effects were abolished by administering glibenclamide. Similarly, the beneficial effects of pravastatin were abolished by administering glibenclamide, implicating K_{ATP} channels as the relevant target. Activation of K_{ATP} channels by pravastatin administration can attenuate ventricular remodeling through a S6 kinase-dependent pathway after infarction.

Key words arrhythmia – ion channels – remodeling – statins

Introduction

Cardiac remodeling is an unfavorable evolution associated with myocardial hypertrophy following myocardial infarction (MI) [50]. On the cellular level, the hypertrophic phenotype is characterized by an increase in cell size. There is considerable evidence that electrophysiological changes are associated with the hypertrophied myocardium [31]. Hypertrophied myocardium has been shown to generate arrhythmias more readily than normal tissue. Agents with the regression of ventricular hypertrophy have been shown to decrease the susceptibility of ventricular arrhythmias [3].

Cardiac remodeling is a complex process involving numerous signaling pathways. Pharmacological therapies, such as angiotensin-converting enzyme inhibitors and β-blockers through different molecular targets,

BRC 628

have been used to prevent cardiac remodeling [7]. Saeed et al. [35] have shown that left ventricular (LV) remodeling is prevented after nicorandil treatment, implying that myocardial ATP-sensitive potassium (K_{ATP}) channels may play a role in ventricular remodeling after infarction. However, the study did not indicate a direct relationship between the activation of K_{ATP} channels and LV remodeling by administering K_{ATP} channel antagonists. Cabo et al. [6] have shown a marked reduction of the current density of potassium current in the border zone cells compared to those in remote sites. Activation of K_{ATP} channels has been shown to attenuate cardiac hypertrophy by inhibition of 70-kDa S6 kinase [36], a key trigger of protein synthesis for hypertrophic changes. Although we have demonstrated cardioprotection against infarct of any size and myocardial ischemia by activation of K_{ATP} channels in animals [18, 46] and in humans [16, 19] in acute settings, the observed beneficial effects do not provide information on whether similar effects would be present on ventricular remodeling with long-term administration.

Epidemiological studies have demonstrated that the benefit of statin treatment after MI extends to patients with normocholesterolemia [32]. Statins exert pleiotropic properties and interfere with signal pathways for hypertrophy, effects that may contribute to their beneficial effects on ventricular remodeling after MI [51]. We [20] and others [44] have shown that statins can activate K_{ATP} channels by increasing the levels of adenosine and nitric oxide, important mediators to trigger opening of K_{ATP} channels. Thus, it is of great interest to assess whether chronic administration of pravastatin can provide beneficial ventricular remodeling by attenuated expression of p70S6 kinase through a K_{ATP} channel-dependent pathway. The purpose of this study was to investigate the effect of pravastatin on cardiomyocyte sizes and the role of myocardial K_{ATP} channels in a normocholesterolemic rat MI model. To confirm that the attenuation of pravastatin-induced myocyte hypertrophy was due to the activation of the K_{ATP} channels, the effect was also investigated in the presence of glibenclamide, a K_{ATP} channel blocker.

Methods

Animals

Male normocholesterolemic Wistar rats (300–350 g) were subjected to ligation of the anterior descending artery, resulting in infarction of the LV free wall. Rats were randomly assigned into 6 groups so as to have approximately the same number of survivors in each group: (1) vehicle group; (2) nicorandil (0.1 mg/kg per day, Chugai Pharmaceutical Co., Japan), a K_{ATP} channel agonist; (3) pravastatin (5 mg/kg per day, Sankyo Co., Japan); (4) glibenclamide (1.4 mg/kg per day), a K_{ATP} channel blocker; (5) a combination of nicorandil and glibenclamide; and (6) a combination of pravastatin and glibenclamide. The doses of nicorandil [9], pravastatin [47], and glibenclamide [1] used in this study have been shown to specifically activate K_{ATP} channels without interfering with hemodynamics. The drugs were given orally by gastric gavage once a day. The drugs were started 24 hours after MI, during which drugs can maximize benefits in this window frame [52] and minimize the possibility of a direct effect on infarct size. In each group treated, drugs were withdrawn about 24 hours before the end of the experiments in order to eliminate their pharmacological actions. The study duration was designed to be 4 weeks because most of the myocardial remodeling process in the rat (70–80 %) is complete within 3 weeks [29]. To prevent hypoglycemic attacks during the administration of glibenclamide, glucose was supplied and frequent glucose examinations were performed by the one-touch method. Sham operation served as controls to exclude the possibility of drugs themselves directly to alter cardiomyocyte hypertrophy. All procedures were in accordance with the Guide for the Care and Use of Laboratory Animals (NIH Publication No. 85–23, revised 1996).

Experimental MI

To create the model, rats were anesthetized with ketamine (90 mg/kg) intraperitoneally. After adequate anesthesia the anterior descending artery ligation between the pulmonary outflow tract and the left atrium or sham operation was performed as described previously [17]. Mortality in the animals with MI was ~50 % within the first 24 hours. None of the sham-operated animals died.

Twenty-eight days after the first operation, the second operation was performed. Using a 2F micromanometer-tipped catheter (Model SPR-407, Miller Instruments, Houston, TX) inserted through the right carotid artery, we measured LV systolic and diastolic pressure as the mean of measurements of five consecutive pressure cycles. The maximal rate of left ventricular pressure rise (+ dP/dt) and decrease (-dP/dt) was measured. Next, the heart was rapidly excised and suspended for retrograde perfusion with a Langendorff apparatus. At completion of the electrophysiological tests, the heart was then rapidly divided into right and left atria, right ventricles and LV, and the scarred area. Each tissue was then weighed individually. To evaluate the degree of pulmonary edema, lungs were also weighed. Samples of the LV from the border zone (0 to 2 mm outside the infarct) were cut transmurally to include all layers from the epi- to the endocardium, were frozen rapidly in liquid nitrogen, and stored at –80 °C until use. Infarct size (%) was expressed as the ratio of the sum of

external and internal perimeters of LV as described by Pfeffer et al. [29]. It has been shown that hypertrophy of the residual myocardium progresses after MI, if infarct size is larger than 30 % of the LV [29]. Thus, with respect to clinical importance, only rats with infarction larger than 30 % of the LV were selected for analysis.

Spontaneous and induced arrhythmias

After isolation, each heart was perfused with a noncirculating modified Tyrode's solution containing (in mmol/L): NaCl 117.0, $NaHCO_3$ 23.0, KCl 4.6, NaH_2PO_4 0.8, MgCl2 1.0, CaCl2 2.0, and glucose 5.5, equilibrated at 37 °C and oxygenated with a 95 % O_2–5 % CO_2 gas mixture. The perfusion medium was maintained at a constant temperature of 37 °C with a roller pump at a constant flow of 4 ml/min. Epicardial electrograms were recorded by an atraumatic unipolar electrode, placed on the epicardial surface of the right atrium and anterior LV wall 2 mm below the circumflex artery. A bipolar pacing electrode was placed near the apex of the heart on the anterior epicardial surface of the right ventricle. Atrial and ventricular epicardial electrocardiograms were continuously displayed on a computerized data acquisition system (Biopac MP100WS).

The hearts were observed for 20 minutes to allow stabilization of contraction and rhythm. The protocol for pacing was modified from that of Belichard et al. [3]. Stimulation intensity was twice the threshold, and stimulus length was 5 ms. Induction of ventricular arrhythmias was then attempted by ventricular stimulation at a basic cycle length of 150 ms (S_0) with single (S_1), double (S_2), and triple (S_3) extrastimuli delivered after 8 paced beats. The end point of ventricular pacing was induction of ventricular tachyarrhythmia. A preparation was considered non-inducible when pacing produced either no ventricular premature contraction or only self-terminating salvos of < 6 beats. Ventricular tachyarrhythmias including ventricular tachycardia and ventricular fibrillation were considered nonsustained when it lasted ≤ 15 beats and sustained when it lasted > 15 beats. An arrhythmia scoring system was modified as previously described [25]: 0, noninducible preparations; 1, nonsustained tachyarrhythmias induced with 3 extrastimuli; 2, sustained tachyarrhythmias induced with 3 extrastimuli; 3, nonsustained tachyarrhythmias induced with 2 extrastimuli; 4, sustained tachyarrhythmias induced with 2 extrastimuli; 5, nonsustained tachyarrhythmias induced with 1 extrastimulus; 6, sustained tachyarrhythmias induced with 1 extrastimulus; and 7, tachyarrhythmias induced during the 8 paced beats. If the heart stopped before the pacing, the arrhythmia score assigned to that heart was 8. When multiple forms of arrhythmias occurred in one heart, the highest score was used. The experimental protocols were typically completed within 10 minutes. Pilot studies revealed no significant tissue edema during the time period required to complete these experiments.

Real-time RT-PCR of p70S6 kinase

To further confirm the downstream activation of K_{ATP} channels, mRNA levels of p70S6 kinase was measured by real-time quantitative reverse transcription-polymerase chain reaction (RT-PCR) from samples obtained from the border zone with the TaqMan system (Prism 7700 Sequence Detection System, PE Biosystems) as our previous description [17]. For p70S6 kinase the primers were sense, 5'-GAAGATTTATTGGTAGCCCACGAA-3'; antisense, 5'-GCACCTCGTCCCCAGAAA-3'. For glyceraldehydes-3-phosphate-dehydrogenase (GAPDH) the primers were 5'-CTTCACCACCATGGAGAAGGC-3' and 5'-GGCATGGACTGTGGTCATGAG-3'. For quantification, p70S6 kinase expression was normalized to the expressed housekeeping gene GAPDH. Reaction conditions were programmed on a computer linked to the detector for 40 cycles of the amplification step.

Western blot analysis of p70S6 kinase

Samples from the border zone were homogenized with a kinametic polytron blender in 100 mM Tris HCl, pH 7.4, supplemented with 20 mmol/L EDTA, 1 mg/ml pepstatin A, 1 mg/ml antipain, and 1 mmol/L benzamidin. Homogenates were centrifuged at 10,000 g for 30 min to pellet the particulate fractions. The supernatant protein concentration was determined with the BCA protein assay reagent kit (Pierce). Twenty μg protein was separated by 8 % SDS-PAGE and electrotransferred onto a nitrocellulose membrane. After incubation with rabbit polyclonal anti-phosphorylated-p70S6 kinase antibodies (Cell Signalling, Hitchin, Kent), the nitrocellulose membrane was then rinsed with a blocking solution and incubated for 2 hours at room temperature. Antigen-antibody complexes were detected with 5-bromo-4-chloro-3-indolyl-phosphate and nitroblue tetrazolium chloride (Sigma). Prestained low molecular weight markers were used to identify the electrophoretic mobility of p70S6 kinase. Films were volume-integrated within the linear range of the exposure using a scanning densitometer. Experiments were replicated three times and results expressed as the mean value.

Immunohistochemical analysis

It has been shown that activation of K_{ATP} channels is associated with attenuated 70-kDa S6 kinase [36]. To confirm the downstream pathways of the K_{ATP} channel, im-

munohistochemical staining of 70-kDa S6 kinase was performed on LV muscle at the border zone. Hearts were snap-frozen in liquid nitrogen, embedded in OCT compound (Tissue-Tek), and cryosections were performed at a thickness of 5 μm. The slides containing the sectioned tissues were fixed in 10 % formalin and rinsed in PBS. Sections were immersed in 3 % H_2O_2 for 12 min at room temperature for blocking endogenous peroxidase activity. Sections were blocked with 10 % normal goat serum in PBS for 15 min. Tissues were incubated with a rabbit polyclonal anti-S6 kinase antibody (Santa Cruz Biotechnology, CA) at dilution 1:10 in 1 % normal goat serum in PBS overnight at 4 °C. Immunostaining with 70-kDa S6 kinase antibodies was performed using a standard immunoperoxidase technique (N-Histofine Simple Stain Rat MAX PO kit, Nichirei Co., Tokyo, Japan). Isotype-identical directly conjugated antibodies served as a negative control.

Cell isolation

Because cardiac hypertrophy is a combination of reactive fibrosis and myocyte hypertrophy, we measured cardiomyocyte sizes at the border zone instead of using myocardial weight to avoid the interference of non-myocytes on post-infarction hypertrophy. Since the molecular measurement procedure does not permit quantitation of cardiomyocyte sizes, additional groups of rats were infarcted using the same procedures and used for measurement of cell sizes at the end of the study (Fig. 1). Myocytes were enzymatically isolated with collagenase (type II; Sigma Chemical Co., St, Louis, MO, USA) and protease (type XIV, Sigma) according to previously described techniques [17]. The undigested infarct area was removed, and the border zone (0 to 2 mm outside the infarct) and remote zone (> 2 mm outside the infarct) were mechanically dispersed. Random high-power fields of the rod-like relaxed myocytes with clear striations were selected to eliminate selection bias. In the sham-operated group, cell width and length were measured from the LV free wall for comparisons. At least 100 cells from each section were selected for measurement of cell length, width and area, and the mean value was used as the individual value for each section. Although it is impossible to isolate myocytes from hearts subjected to molecular study, infarct size should be considered to be similar within various groups because animals were randomly assigned to electrophysiological or molecular study.

Laboratory measurements

To determine the confounding roles of glucose, insulin and cholesterol in ventricular remodeling, blood samples from the aorta were assayed at the end of the study. The plasma insulin concentration was measured by collecting 4 ml of blood in test tubes containing 2 % ethylenediaminetetraacetic acid (80 μl/ml of blood). Blood samples were immediately centrifuges at 3,000 g for 10 min, and the plasmas were stored at –70 °C until further analysis. Insulin was measured by ultrasensitive rat enzyme immunoassay (Mercodia, Uppsala, Sweden).

Statistical analysis

Results were presented as mean ± SD. Statistical analysis was performed using the SPSS statistical package (SPSS, version 10.0, Chicago, IL). A two-way ANOVA was used to search for possible effects of nicorandil, pravastatin and glibenclamide on the measurements of hemodynamics, cholesterol levels, myocyte sizes and, if an F value was found to be significant, a two-tailed Student's t-test for paired observation with Bonferroni's correction was used to test differences. Electrophysiological data (scoring of programmed electrical stimulation-induced arrhythmias) were compared by a Kruskal-Wallis test followed by a Mann-Whitney test. The interaction term of pravastatin and glibenclamide effects was incorporated into the model. The significant level was assumed at value of $P < 0.05$.

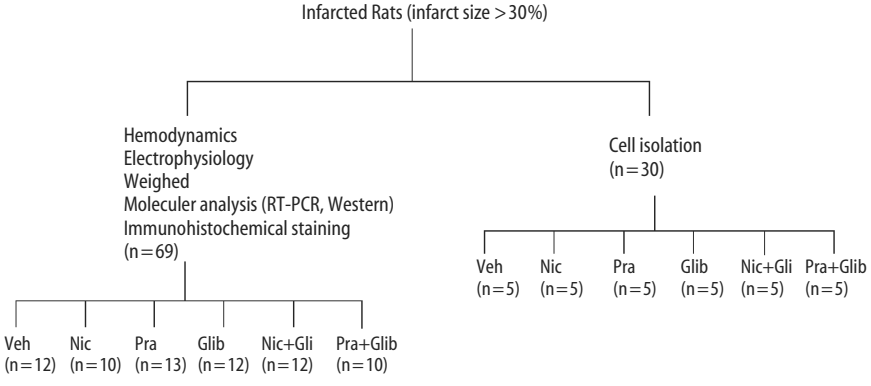

Fig. 1 Flow chart for rats with infarct size > 30 %

Results

Differences in mortality between vehicles (n = 3, 20 %) and treated groups (n = 18, 24 %) were not found throughout the study. No sham-operated rats had evidence of cardiac damage. Pravastatin did not lower serum cholesterol in rats (Table 1), consistent with the notion that compensatory increases in hepatic enzyme production were observed in rats treated with statins [8]. These data indicated the nonlipid effect of pravastatin on ventricular remodeling. Blood pressure, heart rate, infarct size, and glucose levels did not differ between the infarcted groups. Insulin concentrations were significantly increased in rats administered with glibenclamide.

Morphometric studies

In the sham-operated rats, treatment with either nicorandil, pravastatin or glibenclamide had little effect on cardiac gross morphology, whereas there were significant effects on the cardiac morphology after MI (Table 1). Four weeks after MI, the infarcted area of the LV was very thin and was totally replaced by fully differentiated scar tissue. The vehicle-, glibenclamide-, and a combination of nicorandil and glibenclamide- or pravastatin and glibenclamide-treated groups had an increase in right ventricular weight/body weight ratio, and lung weight/body weight ratio compared with sham-operated rats. The weight of the LV inclusive of the septum remained essentially constant 4 weeks after coronary artery occlusion among the infarcted groups.

To characterize the cardiac hypertrophy on a cellular level, we isolated cardiomyocytes from the differently treated groups (Table 2), a more reliable method to quantify the cardiomyocyte size than analysis of tissue section [10]. The cells isolated from the border zone in the vehicle group significantly increased by 70% compared with those from the same area of sham-operated hearts (4582 ± 252 μm^2 in the vehicle group vs. 2685 ± 230 μm^2, $p < 0.0001$). Nicorandil and pravastatin reduced cell areas 23 % and 29 % compared with the vehicle group (both $p < 0.0001$, respectively). The cell width, and length of the pravastatin-treated myocytes were significantly smaller than vehicles (13 %, and 20 %, both $p < 0.05$). The characteristics of cardiomyocytes from remote sites were distinct from the border zones. Compared with border zones, cardiomyocytes from remote sites had smaller sizes in myocyte length, and width in infarcted groups treated with vehicle, glibenclamide, nicorandil + glibenclamide, and pravastatin + glibenclamide.

Table 1 Cardiac morphometry, hemodynamics, and levels of cholesterol, glucose and insulin at the end of study

	Sham						Infarction treated with					
Parameters	Vehicle	Nic	Pra	Glib	Nic + Glib	Pra + Glib	Vehicle	Nic	Pra	Glib	Nic + Glib	Pra + Glib
No. of rats	12	12	12	12	12	12	12	10	13	12	12	10
Body weight, g	403 ± 16	415 ± 23	402 ± 20	405 ± 22	406 ± 16	402 ± 21	396 ± 24	412 ± 16	414 ± 13	412 ± 19	409 ± 20	414 ± 16
HR, bpm	421 ± 14	429 ± 20	417 ± 19	415 ± 23	419 ± 19	442 ± 13	419 ± 21	422 ± 18	424 ± 21	419 ± 17	425 ± 23	423 ± 15
LVESP, mm Hg	115 ± 11	105 ± 9	113 ± 10	107 ± 10	105 ± 12	112 ± 11	109 ± 9	101 ± 6	102 ± 9	105 ± 9	104 ± 9	100 ± 5
LVEDP, mm Hg	6 ± 1	5 ± 2	4 ± 2	6 ± 3	5 ± 1	5 ± 3	19 ± 2[a]	15 ± 4[a]	15 ± 3[a]	20 ± 4[a]	19 ± 3[a]	20 ± 5[a]
LVW/BW, mg/g	2.29 ± 0.18	2.15 ± 0.25	2.30 ± 0.32	2.21 ± 0.25	2.45 ± 0.28	2.34 ± 0.30	3.03 ± 0.25[a]	2.94 ± 0.41[a]	2.95 ± 0.35[a]	3.37 ± 0.48[a]	3.25 ± 0.28[a]	3.38 ± 0.42[a]
RVW/BW, mg/g	0.58 ± 0.09	0.55 ± 0.09	0.58 ± 0.11	0.57 ± 0.09	0.60 ± 0.07	0.58 ± 0.08	0.72 ± 0.15[a]	0.58 ± 0.08[b]	0.60 ± 0.07[c]	0.75 ± 0.12[a]	0.74 ± 0.07[a]	0.76 ± 0.06[a]
LungW/BW, mg/g	4.02 ± 0.32	4.17 ± 0.50	4.23 ± 0.42	4.16 ± 0.32	4.19 ± 0.51	4.23 ± 0.35	5.76 ± 0.43[a]	4.43 ± 0.32[b]	4.58 ± 0.29[c]	5.28 ± 0.42[a]	5.39 ± 0.26[a]	5.45 ± 0.27[a]
+dp/dt, mm Hg/s	7653 ± 763	8693 ± 583	7684 ± 473	8093 ± 634	8436 ± 483	8293 ± 482	4173 ± 428[a]	4482 ± 368[a]	4582 ± 389[a]	3934 ± 326[a]	3672 ± 305[a]	3422 ± 320[a]
–dp/dt, mm Hg/s	5873 ± 563	5073 ± 384	4983 ± 593	5483 ± 683	5092 ± 439	5342 ± 583	3092 ± 381[a]	3762 ± 262[a]	3822 ± 212[a]	2903 ± 298[a]	2738 ± 283[a]	2128 ± 274[a]
Infarct size, %	–	–	–	–	–	–	42 ± 3	41 ± 3	41 ± 5	41 ± 4	44 ± 5	42 ± 5
Cholesterol, mg/dl	41 ± 5	42 ± 10	45 ± 9	41 ± 11	38 ± 9	40 ± 7	40 ± 4	42 ± 10	39 ± 5	45 ± 10	41 ± 9	43 ± 12
Glucose, mg/dl	91 ± 6	90 ± 5	87 ± 7	88 ± 10	93 ± 12	85 ± 10	88 ± 9	92 ± 7	89 ± 10	88 ± 12	94 ± 8	90 ± 5
Insulin, μu/mL	20 ± 9	24 ± 11	26 ± 13	78 ± 15	89 ± 17	92 ± 12	45 ± 15[a]	63 ± 15[a]	57 ± 9[a]	138 ± 19[a]	147 ± 20[a, d]	155 ± 20[a, e]

Values are mean ± SD. *BW* body weight; *Glib* glibenclamide; *HR* heart rate; *LungW* lung weight; *LVEDP* left ventricular end-diastolic pressure; *LVESP* left ventricular end-systolic pressure; *LVW* left ventricular weight; *Nic* nicorandil; *Pra* pravastatin; *RVW* right ventricular weight. [a] $p < 0.05$ compared with the respective groups without infarction; [b] $p < 0.05$ compared with infarcted groups treated with vehicle and nicorandil + glibenclamide; [c] $p < 0.05$ compared with infarcted groups treated with vehicle and pravastatin + glibenclamide; [d] $p < 0.05$ compared with the nicorandil-treated group; [e] $p < 0.05$ compared with the pravastatin-treated group

Table 2 Characteristics of isolated cardiomyocytes

Parameters	Infarction treated with						
	Sham	Vehicle	Nic	Pra	Glib	Nic + Glib	Pra + Glib
Number of animals	5	5	5	5	5	5	5
Border zone							
Myocyte length, μm	129±11	182±21[a]	145±17[a, b]	142±20[a, b]	174±22[a]	170±23[a]	179±14[a]
Myocyte width, μm	20±3	24±3[a]	21±4[b]	21±3[b]	25±5[a]	26±4[a]	26±3[a]
Measured myocyte areas, μm^2	2685±230	4582±252[a]	3537±243[a, b]	3265±206[a, b]	4473±329[a]	4565±364[a]	4930±317[a]
Remote zone							
Myocyte length, μm	132±11	139±22[c]	136±19	137±20	149±24[c]	145±15[c]	145±21[c]
Myocyte width, μm	21±3	22±3	20±4	20±3	22±3[c]	24±4	22±2[c]
Measured myocyte areas, μm^2	2768±272	3062±295[c]	2884±362	2939±312	3457±263[c]	3421±244[c]	3306±253[c]

Values are mean ± SD. *BW* body weight; *Glib* glibenclamide; *HR* heart rate; *LungW* lung weight; *LVEDP* left ventricular end-diastolic pressure; *LVESP* left ventricular end-systolic pressure; *LVW* left ventricular weight; *Nic* nicorandil; *Pra* pravastatin; *RVW* right ventricular weight. [a] $p < 0.05$ compared with the sham-operated group; [b] $p < 0.05$ compared with the vehicle-, glibenclamide-, and combination-treated groups; [c] $p < 0.05$ compared with respective data from border zones within the same group

Electrophysiological stimulation

To further elucidate the physiological effect of attenuated cardiomyocyte hypertrophy, ventricular pacing was performed. Arrhythmia scores in sham-operated rats were very low (0) (Fig. 2). In contrast, ventricular tachyarrhythmias consisting of ventricular tachycardia and ventricular fibrillation were inducible by programmed stimulation in rats with MI. Nicorandil and pravastatin administration significantly decreased the inducibility of ventricular tachyarrhythmias compared with the vehicle group. Glibenclamide administration significantly increased the arrhythmia scores in pravastatin-treated rats compared with the pravastatin-treated rats alone.

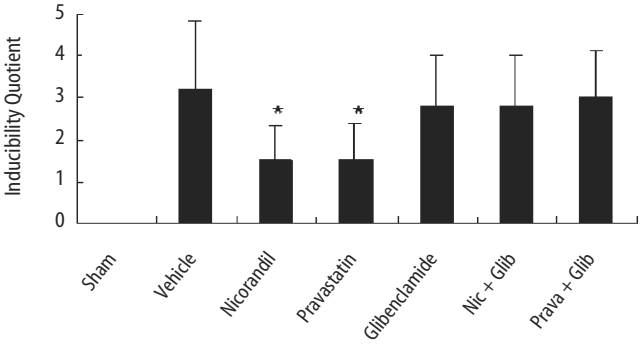

Fig. 2 Inducibility quotient of ventricular arrhythmias by programmed electrical stimulation 4 weeks after MI. * $p < 0.05$ compared with infarcted groups treated with vehicle, glibenclamide, nicorandil (Nic)+glibenclamide (Glib), and pravastatin (Pra)+glibenclamide (Glib)

Immunohistochemical analyses, Western blot, and real-time PCR of p70S6 kinase

Immunohistochemical analysis of the infarcted myocardium revealed the presence of p70S6 kinase immunoreactivity in the myocardial tissue (Fig. 3). Stronger p70S6 kinase signals at the border zone of vehicle-treated rats were observed than in the same region of sham rats. The intensity of the immunoreaction was reduced in the nicorandil- and pravastatin-treated groups compared with that of the vehicle group. Pravastatin-induced beneficial effects were reversed by the addition of glibenclamide, implicating K_{ATP} channels as the relevant target.

Western blot shows that LV p70S6 kinase levels were significantly upregulated 1.9-fold at the border zone in the vehicle-treated rats compared to the sham-operated rats ($p < 0.0001$, Fig. 4). Compared with vehicle-treated rats, LV p70S6 kinase levels in nicorandil- and pravastatin-treated rats were significantly lower at the border zone.

The mRNA levels of p70S6 kinase showed a 2.3-fold upregulation at the border zone in the vehicles compared with the sham-operated rats ($p < 0.0001$, Fig. 5). Compared with vehicle-treated rats, LV p70S6 mRNA levels in nicorandil- and pravastatin-treated rats were significantly lower at the border zone. Thus, the mRNA levels of p70S6 kinase changed in parallel to the tissue peptide levels, implying that the production of p70S6 kinase mRNA is a critical regulation step for its local activation.

Discussions

This study demonstrates for the first time that chronic treatment for 4 weeks with pravastatin leads to favorable ventricular remodeling accompanied by inhibition of pacing-induced ventricular arrhythmias independent of lipid profiles. The attenuated effect of pravastatin on cardiomyocyte hypertrophy was completely prevented in the presence of glibenclamide, which indicates that

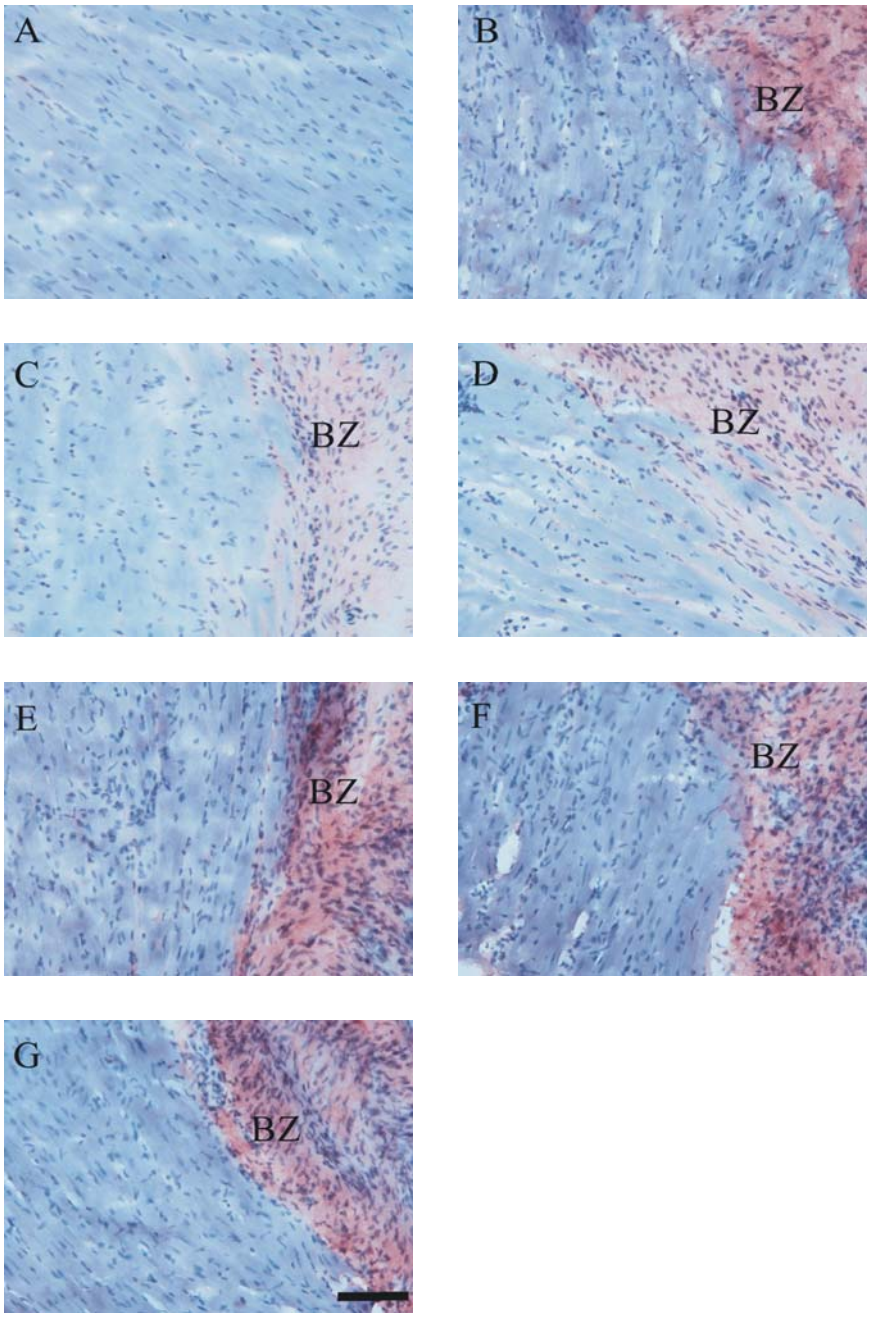

Fig. 3 Immunohistochemical microscopy of 70-kDa S6 kinase (magnification 200X) at the border zone (BZ) in different treated rats. **A** sham-operated group; **B** infarction treated with vehicle; **C** infarction treated with nicorandil; **D** infarction treated with pravastatin; **E** infarction treated with glibenclamide; **F** infarction treated with nicorandil + glibenclamide; and **G** infarction treated with pravastatin + glibenclamide. Positive staining for 70-kDa S6 kinase (brown color) in myocytes was significantly higher in groups treated with vehicle, glibenclamide, and a combination of nicorandil + glibenclamide and pravastatin + glibenclamide than that in sham-operated, nicorandil-treated, and pravastatin-treated rats. The line length corresponds to 200 μm

the effect was related to the K_{ATP} channels. The presence of 70-kDa S6 kinase at these subcellular sites is consistent with a role of K_{ATP} channels in restructuring. These new observations strengthen the concept that K_{ATP} channels play a central role in the remodeling process and may improve our understanding of the beneficial effect of early administration of statins in postinfarction remodeling.

Mechanisms

It appears from our study that the attenuated myocyte hypertrophy is related to a cholesterol-independent activation of K_{ATP} channels in response to statin treatment. The addition of glibenclamide to pravastatin-treated rats impaired their ability to attenuate cellular hypertrophy, implying that this effect is not a nonspecific action. The mechanisms by which pravastatin attenuates cardiac hypertrophy remain to be defined. However, several factors can be excluded: 1) Hemodynamics: Pravas-

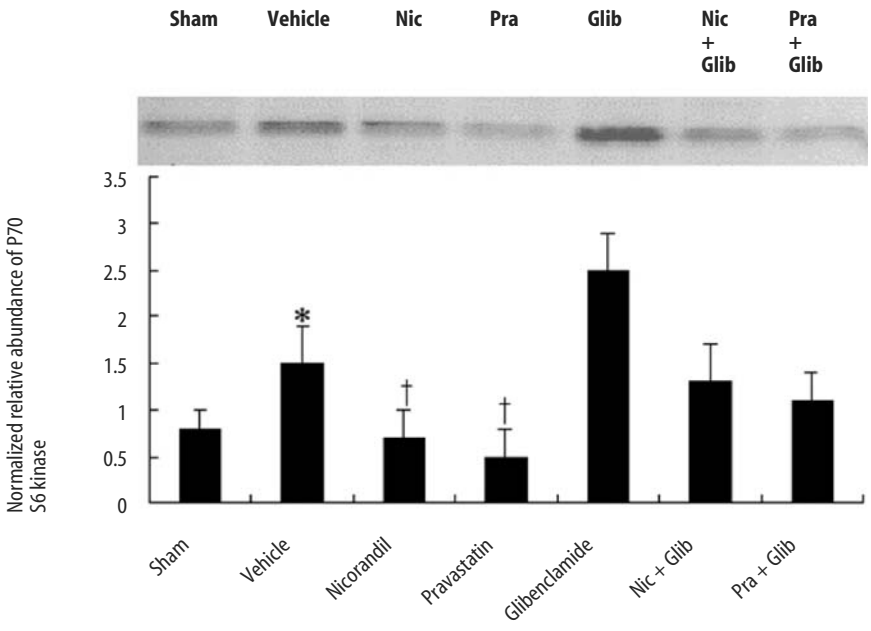

Fig. 4 **A** Western blot analysis of p70S6 kinase showing the effect of KATP channel agonists on immunorecognition of p70S6 kinase in homogenates of the LV from the border zone. Ventricular remodeling was associated with marked increase of p70S6 kinase. Significantly reduced p70S6 kinase was found in the groups treated with either nicorandil (Nic) or pravastatin (Pra) administration compared with control. **B** Densitometric quantification of blot band intensities for relative p70S6 kinase normalized to β-actin (mean ± SD). * $p < 0.05$ compared with sham; † $p < 0.05$ compared with rats treated by combination with glibenclamide, respectively

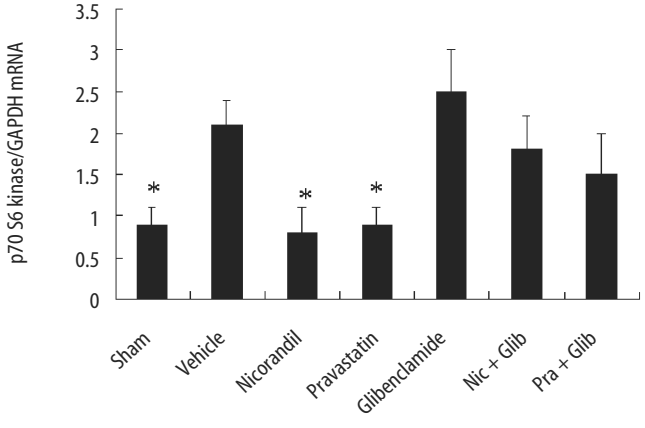

Fig. 5 Left ventricular p70S6 kinase mRNA expression of the sham, and the rats treated with vehicle, nicorandil, pravastatin, glibenclamide, nicorandil + glibenclamide, and pravastatin + glibenclamide. Each mRNA was corrected for an mRNA level of GAPDH. Each column and bar represents mean ± SD. * $p < 0.05$ compared with vehicle-, glibenclamide-, nicorandil + glibenclamide-, and pravastatin + glibenclamide-treated groups

tatin did not exert any hemodynamic effects at the dose used in this study. Glorioso et al. [11] have shown hemodynamic improvement after a 16-week therapy with pravastatin in hypertensive patients, which was not consistent with our stable hemodynamics throughout the study in pravastatin-treated rats. The discrepancy could be due to differences in protocols, study population, and periods of treatment. Indeed, statins have been shown to decrease elevated but not normal blood pressure [46]. In addition, although we demonstrated that ventricular remodeling after infarction was attenuated by pravastatin treatment, the velocity of relaxation as assessed by -dP/dt max and LV end-diastolic pressure did not improve. It is noteworthy that -dP/dt max does not detect subtle changes of relaxation function [2]. Furthermore, LV end-diastolic pressure was largely dependent on loading conditions [38]. 2) Differences in insulin concentrations: Insulin secretion significantly increases in rats treated with glibenclamide compared with vehicles as shown in this study. Hyperinsulinemia has been shown to enhance cardiac hypertrophy [4]. However, the increased insulin levels cannot be a confounding factor of cardiomyocyte hypertrophy because similar cardiomyocyte sizes were observed in groups treated with vehicle and glibenclamide, suggesting that factors other than insulin may contribute to the pathogenesis of cardiac hypertrophy. 3) Differences in glucose concentrations: Hyperglycemia has been shown to adversely affect cardiomyocyte sizes [26]. However, it is unlikely because blood glucose concentrations remained stable during the course of the experiments. Furthermore, nicorandil improved the degree of cardiomyocyte hypertrophy without significant changes in blood glucose levels.

In the heart, p70S6 kinase can be activated by a variety of hypertrophy inducers including mechanical stretch in vitro and pressure overload in vivo [34, 40]. In this study, the incremental load on the remaining myocytes at the border zone reflects an increase in cardiomyocyte sizes by a combination of pressure and volume overload hypertrophy, reflected by increased myocyte length (35 %) and width (14 %). Treatment with rapamycin, a potent p70S6 kinase inhibitor, completely suppressed p70S6 kinase activation and attenuated cardiac hypertrophy induced by aortic constriction [41].

Previous studies have shown that K_{ATP} channel activation inhibits the p70S6 kinase activities [36]; however, the underlying cellular mechanism of such an associa-

tion is unknown. In the present study, p70S6 kinase was activated at the border zone, and administration of nicorandil and pravastatin attenuated p70S6 kinase as shown by immunohistochemical staining and protein measurement. The K_{ATP} channel is a high-fidelity metabolic sensor that adjusts membrane potential-dependent cell functions to match metabolic state [24]. Agonists of K_{ATP} channels have been shown to cause a decrease in the ratio of subendocardial to epicardial blood flow in normal swine [48]. This effect may be magnified in the postinfarcted remodeled LV, in which coronary flow reserve is impaired and subendocardium increases vulnerability to ischemia [54]. Preferential vasodilation of subendocardial vessels due to the activation of K_{ATP} channels prevented flow redistribution away from subendocardium. Previous studies have shown that the decrease in subendocardial energy/phosphate metabolism is correlated with the extent of LV mass [54]. Furthermore, a recent study showed that mitochondrial ATPase expression and decreased ATP content are impaired at the border zone after MI [12]. The intrinsic property of the bioenergetic changes renders the border zone more sensitive to the effects of K_{ATP} channels. The activation of K_{ATP} channels improved myocardial energy metabolism [24], which significantly reduced the extent of p70S6 kinase phosphorylation.

Other mechanisms

Although the present study suggests that the mechanisms of pravastatin-induced cardioprotection may be related to opening of K_{ATP} channels, other potential mechanisms need to be studied. Blockade of free radicals alleviated the development of cardiac hypertrophy [30]. Pravastatin was shown to inhibit production of free radicals [15]. In addition, blunting of the antitropic effect by pravastatin may also result from attenuation of nitric oxide inhibition. Liu et al. [22] have shown increased LV mass in endothelial nitric oxide synthase knockout mice. Second, concerning the mechanisms involved in the attenuation of pravastatin-induced hypertrophy, it is attractive to also consider a potential role of endothelin-1, a potent growth-promoting peptide. We have demonstrated that pravastatin can attenuate the expression of endothelin-1 at the transcription and translation levels [17]. Complex interactions between endothelin-1, free radicals, nitric oxide, and K_{ATP} channels exist that could affect cardiac hypertrophy. However, the effect of pravastatin was abolished by treatment with glibenclamide, implying a pivotal role of K_{ATP} channels in this phenomenon.

Furthermore, pravastatin can prevent ventricular remodeling by modulation of collagen synthesis, activities of matrix metalloproteinases or changes in cytokines. We have recently demonstrated that pravastatin can prevent ventricular remodeling by attenuating the formation of collagen in healed infarcted rats [21]. Matrix metalloproteinases play an important role in the extracellular matrix remodeling and cardiac fibrosis [27]. Previous studies have demonstrated that matrix metalloproteinases are upregulated in failing hearts and are involved in the development and progression of myocardial remodeling [27]. Statins have been shown to inhibit the activities of matrix metalloproteinases [37] and prevent ventricular remodeling. Furthermore, statins attenuated the production of cytokines such as TNF-α, IL-1β, and IL-6 in the infarcted regions, which contributed to improve LV function [53]. Thus, the beneficial effect of pravastatin on postinfarction remodeling can also result from the attenuation of matrix metalloproteinase activities or cytokines.

Arrhythmias

Our results showed that favorable ventricular remodeling after pravastatin administration has benefits not only in anatomical structures, but also in arrhythmia susceptibility. These cellular alterations are important because the border zone is a region where malignant arrhythmia origins. Spach et al. [42] have shown that cell sizes play a crucial role in modulating electrophysiological responses that occur in response to ventricular remodeling. The hypertrophic growth of the surviving myocytes may create a shift in the sympathovagal balance towards a sympathetic prevalence that leaves the myocardium in greater jeopardy for the development of life-threatening arrhythmias [14].

Clinical implications

After acute MI, patients remain at high risk for recurrent cardiovascular events and mortality [5]. Despite the compelling clinical trial evidence that statins reduce mortality in patients after acute MI [28], the mechanisms involved remain unclear. Our data suggested that attenuation of cardiomyocyte hypertrophy is a major mechanism by which pravastatin reduces susceptibility to ventricular arrhythmias after infarction. The results were consistent with a study, showing that attenuated myocardial hypertrophy is paralleled by changes in the inducibility of ventricular arrhythmias [43]. In view of the association between cardiomyocyte sizes and arrhythmias, it is not unrealistic to anticipate a beneficial effect on antiarrhythmia with longer follow-up. The hypothesis was confirmed by a recent study which shows a beneficial effect of lipid-lowering therapy including statins on the recurrence of fatal ventricular arrhythmias in patients with coronary artery disease [23]. Finally, each signaling molecule has different roles, and ac-

tivation of various signaling molecules in concert mediates the hypertrophic response. S6 kinase mechanism is different from known hypertrophic pathways, such as tyrosine kinase-dependent, MAP kinase-dependent, and PKC-dependent signal pathways [33]. The involvement of S6 kinase in pathogenesis of ventricular hypertrophy after MI explained at least in part why it is hard to completely reverse cardiac remodeling by various kinds of medications in clinical settings when S6 kinase blockade is not involved.

Study limitations

There are some limitations in the present study that have to be acknowledged. First, only one time point after infarction was studied. The immunohistochemical and electrophysiological studies were not performed until 4 weeks after infarction. Future research should identify early events such as myocardial inflammation [49], and trace their progression after administering drugs. Second, although we have shown a beneficial effect of pravastatin on ventricular remodeling, the improvement in survival was not significant. The study was not powered for a survival benefit, and the lack of statistical significance may have resulted from a type II error. Finally, a potential problem with the present study is the use of glibenclamide as an antagonist of K_{ATP} channels when there are many potential nonspecific targets of glibenclamide, including the inhibition of Na + channels and the opening of Ca^2 + channels [13]. Glibenclamide can enhance the resting and stimulation-evoked release of norepinephrine, an effect unrelated to K_{ATP} channel blockade [39]. These alternative effects could confound the interpretation of the present study. Use of a more selective antagonist of K_{ATP} channels, 5-hydroxydecanoate or HMR-1098 [46], would have strengthened the hypothesis.

In conclusion, ventricular remodeling after infarction is a complex process characterized by structural, ionic, and electrophysiological perturbations. Our findings suggest a pathogenetic role of regional K_{ATP} channels in cardiac remodeling after MI. Early intervention with pravastatin after MI can reduce the inducibility of ventricular arrhythmias as a result of attenuated ventricular hypertrophy through activation of K_{ATP} channels pathway. Pravastatin treatment had a neutral effect on mortality. The pharmacological profile of pravastatin gives new perspectives in the early treatment of acute MI.

Acknowledgments This work was supported by the grant of Chi-Mei Medical Center (CMFHT 9501, CMFHR9502, CMFHR9506, and CM-TMU9501) and the grant of National Science Council, Republic of China (NSC 94–2314-B-384–001). We thank In-Ping Cheng, Li-Lan Chien, Yi-Wei Chao, Fang-Chin Lee, Shu-Ping Sun, and Chung-Shang Huang for their excellent technical assistance. Pravastatin was a generous gift from Sankyo Company, Limited, Tokyo, Japan.

References

1. Abd Elaziz MA, Al-Dhawailie AA, Teckle A (1998) The effect of stress on the pharmacokinetics and pharmacodynamics of glibenclamide in diabetic rats. Eur J Drug Metab Pharmacokinet 23:371–376
2. Alipov NN, Izrail'tyan IM, Sokolov AV, Trubetskaya LV, Kuznetsova TE (2001) Comparison of different cardiac relaxation indices. Bull Exp Biol Med 131: 416–420
3. Belichard P, Savard P, Cardinal R, Nadeau R, Gosselin H, Paradis P, Rouleau JL (1994) Markedly different effects on ventricular remodeling result in a decrease in inducibility of ventricular arrhythmias. J Am Coll Cardiol 23: 505–513
4. Belke DD, Betuing S, Tuttle MJ, Graveleau C, Young ME, Pham M, Zhang D, Cooksey RC, McClain DA, Litwin SE, Taegtmeyer H, Severson D, Kahn CR, Abel ED (2002) Insulin signaling coordinately regulates cardiac size, metabolism, and contractile protein isoform expression. J Clin Invest 109:629–639
5. Bhatt DL, Steg PG, Ohman EM, Hirsch AT, Ikeda Y, Mas JL, Goto S, Liau CS, Richard AJ, Rother J, Wilson PW; REACH Registry Investigators (2006) International prevalence, recognition, and treatment of cardiovascular risk factors in outpatients with atherothrombosis. JAMA 295:180–189
6. Cabo C, Boyden PA (2003) Electrical remodeling of the epicardial border zone in the canine infarcted heart: a computational analysis. Am J Physiol 284: H372–H384
7. Cohn JN, Ferrari R, Sharpe N (2000) Cardiac remodeling: concepts and clinical implications-a consensus paper from an International Forum on Cardiac Remodeling. J Am Coll Cardiol 35: 569–582
8. Fears R, Richards DH, Ferres H (1980) The effect of compactin, a potent inhibitor of 3-hydroxy-3-methyglutaryl coenzyme-A reductase activity, on cholesterogenesis and serum cholesterol levels in rats and chicks. Atherosclerosis 35:439–449
9. Garnier-Raveaud S, Faury G, Mazenot C, Cand F, Godin-Ribuot D, Verdetti J (2002) Highly protective effects of chronic oral administration of nicorandil on the heart of ageing rats. Clin Exp Pharmacol Physiol 29:441–448
10. Gerdes AM, Capasso JM (1995) Structural remodeling and mechanical dysfunction of cardiac myocytes in heart failure. J Mol Cell Cardiol27:849–856
11. Glorioso N, Manunta P, Filigheddu F, Troffa C, Stella P, Barlassina C, Lombardi C, Soro A, Dettori F, Parpaglia PP, Alibrandi MT, Cusi D, Bianchi G (1999) Effect of the HMG-CoA reductase inhibitors on blood pressure in patients with essential hypertension and primary hypercholesterolemia. Hypertension 34:1281–1286
12. Hu Q, Wang X, Lee J, Mansoor A, Liu J, Zeng L, Swingen C, Zhang G, Feygin J, Ochiai K, Bransford TL, From A, Bache RJ, Zhang J (2006) Profound bioenergetic abnormalities in peri-infarct myocardial regions. Am J Physiol Heart Circ Physiol (in press)

13. Kim SH, Cho KW, Chang SH, Kim SZ, Chae SW (1997) Glibenclamide suppresses stretch-activated ANP secretion: involvement of K^+_{ATP} channels and L-type Ca^{2+} channel. Pfugers Arch 434: 362–372
14. Lantelme P, Cerutti C, Lo M, Paultre CZ, Ducher M (1998) Mechanisms of spontaneous baroreflex impairment in Lyon hypertensive rats. Am J Physiol 275: R820–R825
15. Lee TM, Chou TF, Tsai CH (2002) Association of pravastatin and left ventricular mass in hypercholesterolemic patients: role of 8-iso-prostaglandin F2 a formation. J Cardiovasc Pharmacol 40: 868–874
16. Lee TM, Chou TF, Tsai CH (2003) Differential role of K_{ATP} channels activated by conjugated estrogens in the regulation of myocardial and coronary protective effects. Circulation 107:49–54
17. Lee TM, Chou TF, Tsai CH (2003) Effects of pravastatin on cardiomyocyte hypertrophy and ventricular vulnerability in normolipidemic rats after myocardial infarction J Mol Cell Cardiol 35: 1449–1459
18. Lee TM, Su SF, Tsai CC, Lee YT, Tsai CH (2000) Cardioprotective effects of 17β-estradiol produced by activation of mitochondrial ATP-sensitive K^+ channels in canine hearts. J Mol Cell Cardiol 32: 1147–1158
19. Lee TM, Su SF, Chou TF, Lee YT, Tsai CH (2002) Loss of preconditioning by attenuated activation of myocardial ATP-sensitive potassium channels in elderly patients undergoing coronary angioplasty. Circulation 105:334–340
20. Lee TM, Su SF, Chou TF, Tsai CH (2001) Effect of pravastatin on myocardial protection during coronary angioplasty and the role of adenosine. Am J Cardiol 88:1108–1113
21. Lee TM, Lin MS, Tsai CH, Chang NC (2006) Additive effects of combined blockade of AT1 receptor and HMG-CoA reductase on left ventricular remodeling in infarcted rats. Am J Physiol 291:H1281–H1289
22. Liu YH, Xu J, Yang XP, Yang F, Shesely E, Carretero OA (2003) Effect of ACE inhibitors and angiotensin II type 1 receptor antagonists on endothelial NO synthase knockout mice with heart failure. Hypertension 39:375–381
23. Mitchell LB, Powell JL, Gillis AM, Kehl V, Hallstrom AP; AVID Investigators (2003) Are lipid-lowering drugs also antiarrhythmic drugs? An analysis of the antiarrhythmics versus implantable defibrillators (AVID) trial. J Am Coll Cardiol 42:81–87
24. Murakami Y, Wu X, Zhang J, Ochiai K, Bache RJ, Shimada T (2002) Nicorandil improves myocardial high-energy phosphates in postinfarction porcine hearts. Clin Exp Pharmacol Physiol 29: 639–645
25. Nguyen T, El Salibi E, Rouleau JL (1998) Postinfarction survival and inducibility of ventricular arrhythmias in the spontaneously hypertensive rat: effects of ramipril and hydralazine. Circulation 98:2074–2080
26. Pang Y, Hunton DL, Bounelis P, Marchase RB (2002) Hyperglycemia inhibits capacitative calcium entry and hypertrophy in neonatal cardiomyocytes. Diabetes 51:3461–3467
27. Peterson JT, Hallak H, Johnson L, Li H, O'Brien PM, Sliskovic DR, Bocan TM, Coker ML, Etoh T, Spinale FG (2001) Matrix metalloproteinase inhibition attenuates left ventricular remodeling and dysfunction in a rat model of progressive heart failure. Circulation 103: 2303–2309
28. Pedersen TR, Faergeman O, Kastelein JJ, Olsson AG, Tikkanen MJ, Holme I, Larsen ML, Bendiksen FS, Lindahl C, Szarek M, Tsai J; Incremental Decrease in End Points Through Aggressive Lipid Lowering (IDEAL) Study Group (2005) High-dose atorvastatin vs usual-dose simvastatin for secondary prevention after myocardial infarction: the IDEAL study: a randomized controlled trial. JAMA 294:2437–2445
29. Pfeffer MA, Braunwald E (1990) Ventricular remodeling after myocardial infarction. Circulation 81:1161–1172
30. Pimentel DR, Amin JK, Xiao L, Miller T, Viereck J, Oliver-Krasinski J, Baliga R, Wang J, Siwik DA, Singh K, Pagano P, Colucci WS, Sawyer DB (2001) Reactive oxygen species mediate amplitude-dependent hypertrophic and apoptotic responses to mechanical stretch in cardiac myocytes. Circ Res 89:453–460
31. Qin D, Zhang ZH, Caref EB, Boutjdir M, Jain P, el-Sherif N (1996) Cellular and ionic basis of arrhythmias in postinfarction remodeled ventricular myocardium. Circ Res 79:461–473
32. Sacks FM, Pfeffer MA, Moye LA, Rouleau JL, Rutherford JD, Cole TG, Brown L, Warnica JW, Arnold JM, Wun CC, Davis BR, Braunwald E (1996) The effect of pravastatin on coronary events after myocardial infarction in patients with average cholesterol levels. N Eng J Med 335:1001–1009
33. Sadoshima J, Izumo S (1995) Rapamycin selectively inhibits angiotensin II-induced increase in protein synthesis in cardiac myocytes in vitro. Potential role of 70-kDa S6 kinase in angiotensin II-induced cardiac hypertrophy. Circ Res 77:1040–1052
34. Sadoshima J, Izumo S (1997) The cellular and molecular response of cardiac myocytes to mechanical stress. Annu Rev Physiol 59:551–571
35. Saeed M, Watzinger N, Krombach GA, Lund GK, Wendland MF, Chujo M, Higgins CB (2002) Left ventricular remodeling after infarction: sequential MR imaging with oral nicorandil therapy in rat model. Radiology 224:830–837
36. Sanada S, Node K, Asanuma H, Ogita H, Takashima S, Minamino T, Asakura M, Liao Y, Ogai A, Kim J, Hori M, Kitakaze M (2002) Opening of the adenosine triphosphate-sensitive potassium channel attenuates cardiac remodeling induced by long-term inhibition of nitric oxide synthesis: role of 70-kDa S6 kinase and extracellular signal-regulated kinase. J Am Coll Cardiol 40:991–997
37. Saka M, Obata K, Ichihara S, Cheng XW, Kimata H, Nishizawa T, Noda A, Izawa H, Nagata K, Murohara T, Yokota M (2006) Pitavastatin improves cardiac function and survival in association with suppression of the myocardial endothelin system in a rat model of hypertensive heart failure. J Cardiovasc Pharmacol 47:770–779
38. Schmiel FK, Lorenzen N, Fischer G, Harding P, Kramer HH (2005) Diastolic left ventricular function. Experimental study of the early filling period using the Voigt model. Basic Res Cardiol 100: 64–74
39. Schotborgh CE, Wilde AAM (1997) Sulfonylurea derivatives in cardiovascular research and in cardiovascular patients. Cardiovasc Res 34:73–80
40. Shioi T, McMullen JR, Tarnavski O, Converso K, Sherwood MC, Manning WJ, Izumo S (2003) Rapamycin attenuates load-induced cardiac hypertrophy in mice. Circulation 107:1664–1670
41. Shioi T, McMullen JR, Tarnavski O, Converso K, Sherwood MC, Manning WJ, Izumo S (2003) Rapamycin attenuates load-induced cardiac hypertrophy in mice. Circulation 107:1664–1670
42. Spach MS, Heidlage JF, Dolber PC, Barr RC (2000) Electrophysiological effects of remodeling cardiac gap junctions and cell sizes. Experimental and model studies of normal cardiac growth. Circ Res 86:302–311
43. St John Sutton M, Lee D, Rouleau JL, Goldman S, Plappert T, Braunwald E, Pfeffer MA (2003) Left ventricular remodeling and ventricular arrhythmias after myocardial infarction. Circulation 107:2577–2582
44. Tavackoli S, Ashitkov T, Hu ZY, Motamedi M, Uretsky BF, Birnbaum Y (2004) Simvastatin-induced myocardial protection against ischemia-reperfusion injury is mediated by activation of ATP-sensitive K^+ channels. Coron Artery Dis 15:53–58

45. Terzoli L, Mircoli L, Raco R, Ferrari AU (2005) Lowering of elevated ambulatory blood pressure by HMG-CoA reductase inhibitors. J Cardiovasc Pharmacol 46:310–315
46. Tsai CH, Su SF, Chou TF, Lee TM (2002) Differential effect of sarcolemmal and mitochondrial K_{ATP} channels activated by 17 b-estradiol on reperfusion arrhythmias and infarct sizes in canine hearts. J Pharmacol Exp Ther 301: 234–240
47. Ueda Y, Kitakaze M, Komamura K, Minamino T, Asanuma H, Sato H, Kuzuya T, Takeda H, Hori M (1999) Pravastatin restored the infarct size-limiting effect of ischemic preconditioning blunted by hypercholesterolemia in the rabbit model of myocardial infarction. J Am Coll Cardiol 34:2120–2125
48. Verdouw PD, Sassen LM, Duncker DJ, Schmeets IO, Rensen RJ, Saxena PR (1987) Nicorandil-induced changes in the distribution of cardiac output and coronary blood flow in pigs. Naunyn Schmiedebergs Arch Pharmacol 336: 352–358
49. Viedt C, Shen W, Fei J, Kamimura M, Hansch GM, Katus HA, Kreuzer J (2003) HMG-CoA reductase inhibition reduces the proinflammatory activation of human vascular smooth muscle cells by the terminal complement factor C5b-9. Basic Res Cardiol 98:353–361
50. Weber KT, Anversa P, Armstrong PW, Brilla CG, Burnett JC Jr, Cruickshank JM, Devereux RB, Giles TD, Korsgaard N, Leier CV (1992) Remodeling and reparation of the cardiovascular system. J Am Coll Cardiol 20:3–16
51. Werner N, Nickenig G, Laufs U (2002) Pleiotropic effects of HMG-CoA reductase inhibitors. Basic Res Cardiol 97: 105–116
52. Xia QG, Chung O, Spitznagel H, Illner S, Janichen G, Rossius B, Gohlke P, Unger T (2001) Significance of timing of angiotensin AT1 receptor blockade in rats with myocardial infarction-induced heart failure. Cardiovasc Res 49: 110–117
53. Zhang J, Cheng X, Liao YH, Lu B, Yang Y, Li B, Ge H, Wang M, Liu Y, Guo Z, Zhang L (2005) Simvastatin regulates myocardial cytokine expression and improves ventricular remodeling in rats after acute myocardial infarction. Cardiovasc Drugs Ther 19:13–21
54. Zhang J, McDonald KM (1995) Bioenergetic consequences of left ventricular remodeling. Circulation 92:1011–1019